

Generic Contrast Agents

Our portfolio is growing to serve you better. Now you have a *choice*.



[VIEW CATALOG](#)

AJNR

This information is current as of May 16, 2025.

Maximum AmbiGuity Distance for Phase Imaging in Detection of Traumatic Cerebral Microbleeds: An Improvement over Current Imaging Practice

K. Nael, J.C. Dagher, M.E. Downs, M.S. Fine, E. Brokaw and D. Millward

AJNR Am J Neuroradiol 2020, 41 (11) 2027-2033

doi: <https://doi.org/10.3174/ajnr.A6774>

<http://www.ajnr.org/content/41/11/2027>

Maximum AmbiGuity Distance for Phase Imaging in Detection of Traumatic Cerebral Microbleeds: An Improvement over Current Imaging Practice

K. Nael, J.C. Dagher, M.E. Downs, M.S. Fine, E. Brokaw, and D. Millward



ABSTRACT

BACKGROUND AND PURPOSE: Developed using a rigorous mathematic framework, Maximum AmbiGuity distance for Phase Imaging (MAGPI) is a promising phase-imaging technique that provides optimal phase SNR and reduced susceptibility artifacts. We aimed to test the potential of MAGPI over routinely used SWI in the detection of traumatic cerebral microbleeds in athletes diagnosed with mild traumatic brain injury.

MATERIALS AND METHODS: In this prospective study, 10 athletes (18–22 years of age, 3 women/7 men) diagnosed with mild traumatic brain injury were enrolled. Brain MRIs were performed using 3T MR imaging at 2 days, 2 weeks, and 2 months after head trauma. The imaging protocol included whole-brain T1 MPRAGE, T2 FLAIR, conventional SWI, and the MAGPI multiecho sequence. Phase images from MAGPI were put through a previously described SWI process to generate MAGPI-SWI. Conventional and MAGPI-SWI were assessed independently by a board-certified neuroradiologist for the presence of contusions and cerebral microbleeds. All participants had routine neuropsychological assessment and Visuo-Motor Tests.

RESULTS: At initial assessment, 4 of the participants had visuo-motor performance indicative of mild traumatic brain injury, and 4 participants had a Post-Concussion Symptom Scale score of >21 , a threshold that has been used to define moderate impairment. Cerebral microbleeds were identified in 6 participants on MAGPI-SWI, 4 of whom had evidence of concurrent contusions on FLAIR imaging. None of these cerebral microbleeds were identified confidently on conventional SWI due to substantial distortion and susceptibility artifacts.

CONCLUSIONS: Optimal phase unwrapping with reduced susceptibility in MAGPI-SWI can clarify small microbleeds that can go undetected with routinely used conventional SWI.

ABBREVIATIONS: CMB = cerebral microbleeds; ImPACT = Immediate Post-Concussion Assessment and Cognitive Testing; MAGPI = Maximum AmbiGuity distance for Phase Imaging; mTBI = mild traumatic brain injury; PCSS = Post-Concussion Symptom Scale; VMT = Visuo-Motor Test

Approximately 75% of patients who sustain traumatic brain injury have had mild traumatic brain injury (mTBI).¹ Eclipsing the economic cost of mTBI (\$18 billion annually) is the profound health and social damage altering the lives of dynamic

individuals: Of 1.2 million patients with mTBI in the United States each year, 400,000 are children and adolescents, 300,000 are athletes, and 25,000 are members of the military.²

At initial assessment, however, most patients with mTBI have normal neuroimaging findings due to the subtle nature of traumatic changes.³ Typical imaging findings in mTBI include nonhemorrhagic small contusions and cerebral microbleeds (CMB).^{4,5}

Histopathologically, CMB represent focal accumulations of hemosiderin-containing macrophages with paramagnetic properties that can result in susceptibility-related signal loss on MR imaging, best depicted by T2*-weighted sequences or SWI.^{6–8}

The introduction of the SWI sequence has resulted in incremental improvement in the detection of CMB compared with traditional T2*-weighted sequences.^{7,9} SWI combines the MR phase signal, in addition to the magnitude, to improve the contrast in the overall image. Despite these recent advances and improvement in the detection of CMB afforded by the increasing

Received June 3, 2019; accepted after revision July 7, 2020.

From the David Geffen School of Medicine (K.N.), University of California, Los Angeles, Los Angeles, California; Emerging Technologies (J.C.D., M.E.D., M.S.F., E.B.), MITRE Corporation, McLean, Virginia; and Athletics Department (D.M.), University of Arizona, Tucson, Arizona.

This work was supported by internal funding from the MITER Corporation.

Paper previously presented at: Annual Meeting of the American Society of Neuroradiology, May 18–23, 2019; Boston, Massachusetts; Abstract 2458 and nominated for the ASNR Cornelius Dyke Award 2019.

Please address correspondence to Kambiz Nael, MD, David Geffen School of Medicine at UCLA, Department of Radiological Sciences, 757 Westwood Plaza, Suite 1621, Los Angeles, CA, 90095-7532; e-mail: Kambiznael@gmail.com; @kambiznael

Indicates open access to non-subscribers at www.ajnr.org

<http://dx.doi.org/10.3174/ajnr.A6774>

Table 1: Data collection schedule

Examination, Procedure Description	Duration (Min)	Visit 1 (2–3 Days)	Visit 2 ^a	Visit 3 (2 Weeks)	Visit 4 (1.5 Months)
Informed consent	15	X			
Demographics questionnaire	5	X			
MRI	35	X		X	X
Visuo-Motor tracking	10	X	X	X	X
ImPACT	25 (10 min for questionnaire only)	Questionnaire only	X	Questionnaire only	Questionnaire only
Total time (min)		75	35	55	55

Note:—X indicates task was performed, for example Visuo-motor tracking was performed in visit 1, 2, 3 and 4.

^aVisit 2: additional data collection was performed during a scheduled follow-up at a point in time determined by team of physicians (usually within 1 day from visit 1).

Table 2: Summary of clinical assessment and imaging findings in all 10 participants with presentation of mTBI

Participant No.	ImPACT (at Visit 2) ^a	PCSS	VMT ^c	FLAIR ^d (Contusions)	SWI ^d (CMB)	MAGPI-SWI ^d (CMB)
1	+	19	—	—	—	—
2	+	38 ^b	+	+	—	+
3	—	15	—	+	—	+
4	+	20	—	~	—	+
5	+	63 ^b	—	—	—	—
6	—	4	—	+	—	+
7	—	37 ^b	+	~	—	+
8	—	21	+	—	—	—
9	—	0	—	—	—	—
10	—	34 ^b	+	+	—	+

^aPlus sign in ImPACT indicates performance indicative of traumatic brain injury.

^bScore >21 indicates a threshold that has been used to define moderate impairment.

^cPlus sign in VMT indicates performance indicative of traumatic brain injury.

^d+ indicates positive imaging finding (contusion on FLAIR) and (CMB on SWI or MAGPI-SWI). — indicates absence of imaging finding. ~ inconclusive evidence of injury on imaging.

use of high-field-strength MR imaging systems and dedicated imaging sequences such as SWI, our current imaging repertoire significantly underestimates the true number of CMB, with an estimated number of false-negative findings in the range of 50% compared with histopathologic analysis.¹⁰ Therefore, there is a pressing need for tools enabling more sensitive measurement of specific mTBI biologic markers.

One of the limitations of SWI is the inherent trade-off in the choice of the TE, which balances phase-image contrast and susceptibility-induced signal loss. While longer TEs are preferable to improve the sensitivity for detection of CMB, they result in increased susceptibility-induced signal-loss artifacts, which will be problematic near skull base structures. Techniques have been developed to address this concern: Multiecho SWI sequences attempt to provide the advantages of both short and long TEs but have suboptimal phase SNR at shorter TEs, phase wrapping at longer TEs, and increased noise due to the larger readout bandwidths required to accommodate multiple echoes in a TR.¹¹ While magnitude images have better SNR at shorter TEs and decay at longer TEs quasi-exponentially, the trade-off is more complex with phase images. With the MR imaging phase, the phase signal buildup is small at short TEs, thus yielding a poor phase SNR, even in the presence of a modest amount of noise. The phase SNR increases with the TE, reaches a maximum, and falls again as the magnitude of SNR decay increases the noise in the phase signal.¹¹ The maximum phase SNR is attained at TE = T2* of

tissue. Normally, the TE for the best phase SNR is chosen at around TE = 30 ms at 3T.^{11,12}

Recently, Maximum AmbiGuity distance for Phase Imaging (MAGPI) has been developed as a promising multiecho phase imaging technique that addresses the trade-offs and concerns above.¹¹ By adopting a rigorous mathematic framework (maximum-likelihood), MAGPI has been shown to provide optimal phase SNR with no phase wrapping and reduced susceptibility artifacts.

We hypothesized that the improved phase image quality of MAGPI has the potential to overcome traditional SNR trade-offs associated with the SWI process.

We tested this hypothesis clinically in the context of detection of traumatic CMB in athletes diagnosed with mTBI.

MATERIALS AND METHODS

Study Design

This was a longitudinal single-center prospective study that was approved by the University of Arizona institutional review board. Ten concussed adult athletes from the University's Athletics Department were enrolled after informed consent was obtained. Participants were then referred to the Athletics Department clinical team for postconcussion evaluation. Data collection took place at the following fixed intervals (visits) after head trauma (Table 1): 1) visit 1 within 2–3 days, 2) visit 2, an additional short data collection performed during a scheduled routine follow-up after concussion at a point in time determined by the team of physicians at the University's Athletic Department (usually within 1 day from visit 1), 3) visit 3 at 2 weeks, and 4) visit 4 at 1.5 months. The estimated overall duration for protocol completion per study participant per visit was approximately 75 minutes (Table 1).

Image Acquisition

Image acquisition was performed using a 3T MR imaging scanner (Magnetom Skyra; Siemens) during visits 1, 3, and 4 following head trauma. The imaging protocol included whole-brain T1 MPRAGE, T2 FLAIR, a conventional SWI sequence (TE = 30 ms, TR = 40 ms, flip angle = 15°, matrix size = 336 × 384 × 112, voxel size = 0.57 × 0.57 × 1.2 mm³, readout bandwidths = 80 Hz/pixel,

generalized autocalibrating partially parallel acquisition = $2\times$ acceleration, acquisition time = 8 minutes 30 seconds), and the MAGPI multiecho sequence (TE = 9.34, 17.29, 22.19, 27.09, 32.12, 37.56 ms; TR = 40 ms; flip angle = 15° ; matrix size = $552 \times 608 \times 72$; voxel size = $0.37 \times 0.37 \times 2 \text{ mm}^3$; readout bandwidths = 220 Hz/pixel; generalized autocalibrating partially parallel acquisition = $3\times$ acceleration; acquisition time = 8 minutes 25 seconds). Note that MAGPI used a high-readout bandwidth to accommodate reading more echoes in the same TR. The acquisition time was kept the same between the single and multiecho sequences.

MAGPI Postprocessing

MR phase images were reconstructed from channel-uncombined multiecho complex data according to a prescription described previously.^{11,13} The reconstruction process was performed on a Linux computer with a GPU and required about 3 minutes to reconstruct the entire brain volume. The MAGPI phase images were subsequently put through the SWI process as previously described.¹⁴ The MAGPI-SWI process has the following differences: Because MAGPI generates channel-combined, phase-unwrapped, denoised phase images, we were able to apply the high-pass filtering required in SWI directly in the phase domain. Therefore, instead of using the previously homodyne filtering process, we applied a version of the bilateral high-pass-filtering process introduced previously.^{14,15} The advantages of such a filter are reduced blooming artifacts around tissue/bone areas.

Because MAGPI phase images inherently have a higher SNR than traditional phase images, we multiplied the phase mask only twice, instead of 4 times as in prior reports, while achieving contrast similar to that of traditional SWI.¹⁴ Multiplying the mask 4 times increases the contrast to include effects from cortical folds and other deeper gray matter structures. Multiplying the mask a lower number of times reduces the noise amplification associated with this operation.¹⁴

To enable a more direct comparison between the postprocessing steps of MAGPI-SWI and traditional SWI, we performed the following additional experiment: Using raw data from the MAGPI sequence, we created high-pass-filtered phase images according to both the traditional SWI process (as described by Haacke et al¹⁴) and the MAGPI-SWI process (as described above). The overall image quality of phase images in terms of delineation of iron-containing structures such as the red nuclei and substantia nigra was evaluated.

Clinical Assessment

A physician performed routine neuropsychologic assessment including Immediate Post-Concussion Assessment and Cognitive Testing (ImpACT questionnaire) and a novel Visuo-Motor Test (VMT).

ImpACT includes a series of tests used to assess cognitive functioning, including attention span, working memory, sustained and selective attention time, response variability, nonverbal problem-solving, and reaction time. The test also records the severity of 22 symptoms via a 7-point Likert scale (Post-Concussion Symptom Scale [PCSS]). All enrolled athletes also had a baseline (preconcussion) ImpACT test by the University's Athletics Department.

In addition, each participant underwent a VMT during every visit. During this visuomotor task, individuals were asked to modulate their grip force, as measured by a hand dynamometer, to match a variable target force, displayed visually on an iPad (Apple).¹⁶ A horizontal line is the target and moves up and down on the screen in a smooth-but-unpredictable manner. Individuals control the height of the vertical white bar by squeezing the dynamometer. Participants are asked to track the target for 3 minutes. Adequate training was provided to each individual before starting the test. The scores of the ImpACT test and the results of the VMT were recorded for each participant and used for analysis.

Image Analysis

Image analysis was performed by a board-certified neuroradiologist who was blinded to the type of SWI studies (conventional versus MAGPI). FLAIR, MAGPI-SWI, and conventional SWI source images (not the minimum-intensity-projection images)¹⁷ were available for detection of cerebral contusions and CMB. Special attention was paid to common areas for cerebral contusions, including the inferior frontal lobe and temporal poles.

In addition, the overall quality of phase images in terms of delineation of iron-containing structures such as the red nuclei and substantia nigra was evaluated using a typical 5-point Likert scale by the same neuroradiologist.

RESULTS

All study participants (18–22 years of age, 3 women and 7 men) were diagnosed with mTBI by a trained clinician. Participants completed 4 assessments at 2.2 ± 0.8 days (visit 1), 1.7 ± 2.1 days (visit 2), 15.2 ± 3.2 days (visit 3), and 44.3 ± 2.9 days (visit 4) after injury. At the initial assessment, participants had an average PCSS score of 25.1 ± 18.5 . Four participants (Nos. 2, 5, 7, and 10) had a PCSS of >21 , a threshold that has been used to define moderate impairment.¹⁸ The most commonly encountered symptom (≥ 3 severity) was fatigue, which was reported by 5 of the participants. At initial assessment, 4 participants (Nos. 2, 7, 8, and 10) had VMT performance indicative of mTBI based on a previously defined threshold.¹⁶ The mean PCSS for these 4 subjects was 32.5 ± 7.85 with 3 having a score of ≥ 21 .

Two weeks postinjury, participants had an average PCSS score of 3.0 ± 6.0 with most (6 of 10) becoming completely asymptomatic at that time. No participants had a PCSS of >21 . VMT performance was reduced below the threshold for 2 of the 4 individuals (only Nos. 8 and 10 remained above the threshold). According to the ImpACT scale, participants 1, 2, 4, and 5 showed signs of injury at this time point compared with baseline, with participants 2, 4, and 5 showing visual memory deficits, participants 1, 3, and 5 showing reaction time deficits, and participant 1 also presenting with visual-motor speed impairment.

Four participants had suspect areas of contusions on FLAIR images, evident by small foci of FLAIR hyperintensity (participants 2, 3, 6, and 10) (Fig 1). These findings persisted on all 3 imaging sessions. The same 4 participants also had indications of CMB on MAGPI-SWI, evident by foci of increased susceptibility. Two other participants (4 and 7) had CMB confirmed on MAGPI-SWI without associated contusions on FLAIR images (Fig 2). None of these CMB were noticed confidently on conventional SWI due to

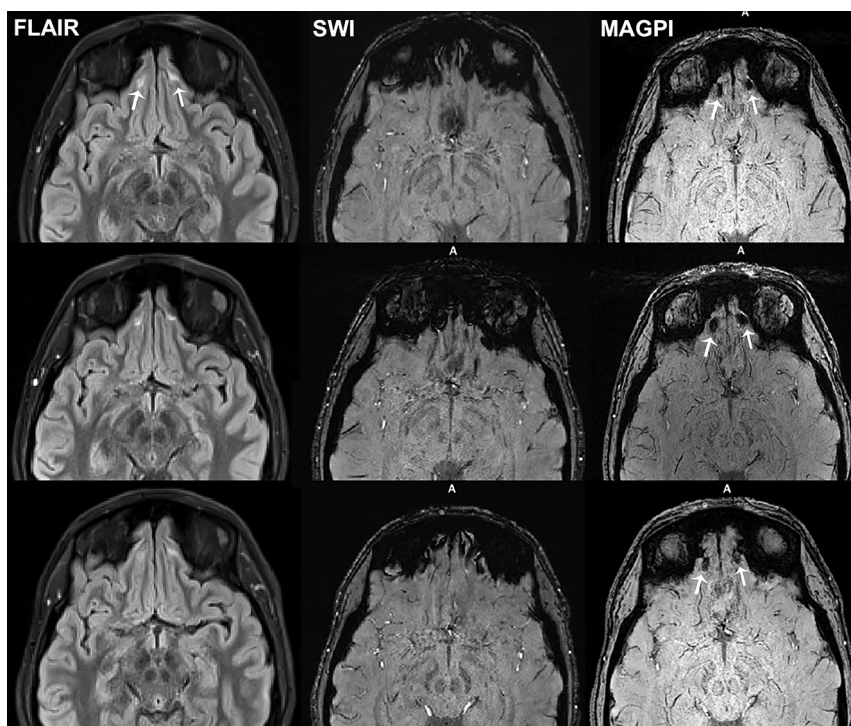


FIG 1. A softball player who had trauma to the forehead and nose (participant 2). The initial Post-Concussion Symptom Scale score was 38. MR images shown are FLAIR, SWI, and MAGPI-SWI obtained at 2 days (upper row), 2 weeks (middle row), and 6 weeks (lower row) after head trauma. There are small contusions in the inferior frontal lobes (arrows on FLAIR). In the same region, there are small foci of microbleeds on the MAGPI-SWI persistent on all 3 visits (arrows on MAGPI). The susceptibility signal on visit 3 (6 weeks after trauma) has slightly decreased. Please note that these microhemorrhages were exaggerated on the traditional SWI due to skull base-related susceptibility artifacts and thus were unnoticed. The Post-Concussion Symptom Scale score was 0 at 6-week follow-up.

substantial distortion and susceptibility artifacts in the region of the gyrus rectus (Figs 1 and 2). The results of clinical assessment and imaging findings are summarized in Table 2.

The image quality of the high-pass-filtered phase images in terms of delineating iron-containing structures was rated consistently higher (median score = 4) on images generated from MAGPI-SWI versus traditional SWI (median score, 2) ($P = .002$) (Fig 3).

DISCUSSION

To the best of our knowledge, this is the first work in which the advantages of MAGPI over phase-processing methods were evaluated in the context of SWI processing. The advantages of MAGPI over traditional phase-unwrapping and phase-processing algorithms in the raw phase domain have been previously reported.^{11,19} The superior performance of MAGPI in terms of phase SNR over other phase-estimation methods was reported in 2016.¹¹ Recently, MAGPI was shown to produce more repeatable and reproducible results than other methods used for phase unwrapping.¹⁹ Taking advantage of these technical improvements, we showed improved clinical performance of MAGPI-SWI in the detection of CMB compared with the currently used commercially available SWI.

CMB can be seen in roughly 30% of mTBI MR images.⁴ In mTBI, CMB can be seen in the inferior frontal and anterior temporal lobes where contusions can commonly occur due to close proximity to the calvaria and skull base. In cases with a history of more severe head trauma, CMB may be seen in deeper structures such as the corpus callosum and deep white matter tracts, often in association with diffuse axonal injury.^{20,21} Because of the paramagnetic hemosiderin and ferritin content, CMB can be detected by MR imaging as hypointense foci, most notably on T2*-weighted imaging.

Because the phase of the MR signal is much more sensitive than its magnitude to electromagnetic effects induced by CMB and iron deposits,^{22,23} SWI was proposed to use this added sensitivity in the phase domain to increase the contrast in the magnitude images.¹⁴ SWI typically uses a 3D high-spatial-resolution gradient recalled-echo sequence with prolonged TEs to enhance the susceptibility contrast. Postprocessing of SWI involves combining magnitude images with high-pass-filtered (homodyne) phase images to enhance the sensitivity for detecting CMB in comparison with conventional gradient recalled-

echo.^{24,25} Some investigators showed an increase of up to 50% in the detection of CMB using SWI over gradient recalled-echo.^{7,9} Despite the promise of SWI, compared with postmortem histopathologic analysis, at least half of CMB can still be missed with premortem clinical MR imaging.¹⁰

The contrast of SWI is limited by the inherent trade-off between phase noise and phase contrast. Specifically, the SWI phase mask generated from the high-pass-filtered phase image is repeatedly multiplied with the magnitude image. As the number of multiplications increases, the contrast from the phase increases, but so does the noise contribution. A balance between phase noise and phase contrast has been reported with around 4 multiplications.¹⁴ In addition to phase noise, other errors that limit the information with SWI are susceptibility-induced phase-wrapping errors, susceptibility-induced signal loss, phase-combination errors in parallel imaging, and phase-offset errors in multiecho sequences. It has been shown that MAGPI, a recently proposed phase estimation, attains optimal phase SNR because it optimally combines multichannel multiecho data in a maximum-likelihood fashion.¹¹ In fact, in this work, we observed overall improved image quality and better delineation of iron-containing structures on the high-pass-filtered phase images from MAGPI-SWI compared with conventional SWI afforded by a higher SNR and contrast-to-noise ratio obtained with MAGPI as reported by prior work using phantom analysis.^{11,13}

We specifically evaluated the performance of MAGPI in regions with susceptibility-induced signal loss related to the close proximity to the skull base such as the inferior frontal and anterior temporal lobes where contusions can commonly occur, and

we showed that MAGPI was able to recover clinical information in these regions. In 4 participants who had cerebral contusions on FLAIR imaging, we were able to identify CMB with MAGPI-SWI but not with the traditional SWI process (Fig 1). In addition,

in 2 other individuals without clear evidence of cerebral contusions on FLAIR imaging, CMB were identified on MAGPI-SWI only (Fig 2). Three of 4 individuals who had evidence of brain injury on VMT (Nos. 2, 7, 8, and 10) and 3 of 4 subjects (Nos. 2, 5, 7, and 10) who had evidence of moderate impairment based on PCSS (PCSS > 21) had CMB on MAGPI-SWI. The clinical and prognostic implications of CMB and patients' symptoms in mTBI are still evolving, and future work is needed.^{26,27}

Note that the gains observed with MAGPI-SWI are due not only to improved phase unwrapping in regions of large phases but also to improved phase SNR throughout the image, especially in regions of signal drop. Applying phase-unwrapping methods alone with traditional SWI would have only modest incremental value in terms of improving image quality²⁸ for the following 3 reasons: First, phase-unwrapping algorithms do not recover signal loss due to susceptibility-induced dephasing. The improved SNR of MAGPI in such areas is the fundamental reason behind its improved ability to detect CMB in this study. Second, the homodyne processing used with SWI

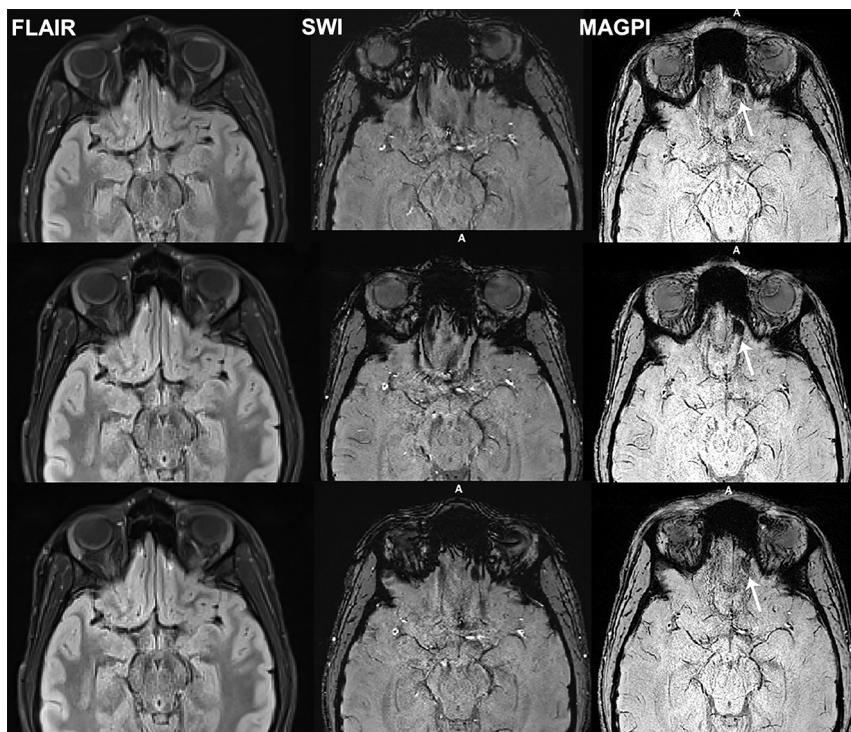


FIG 2. A football player who had helmet-to-helmet frontal trauma (participant 7). The initial postconcussion symptom scale was 37. MR images shown are FLAIR, SWI, and MAGPI-SWI obtained at 2 days (*upper row*), 2 weeks (*middle row*), and 6 weeks (*lower row*) after head trauma. There is a microbleed in the left inferior frontal lobe best seen on MAGPI-SWI (*arrows*). No definitive contusion is visible on FLAIR images. The susceptibility signal on visit 3 (6 weeks after trauma) has slightly decreased in size and intensity. Please note that this microbleed was exaggerated on the traditional SWI due to skull base-related susceptibility artifacts and thus less confidently noticed. The Post-Concussion Symptom Scale score was 0 at 6-week follow-up.

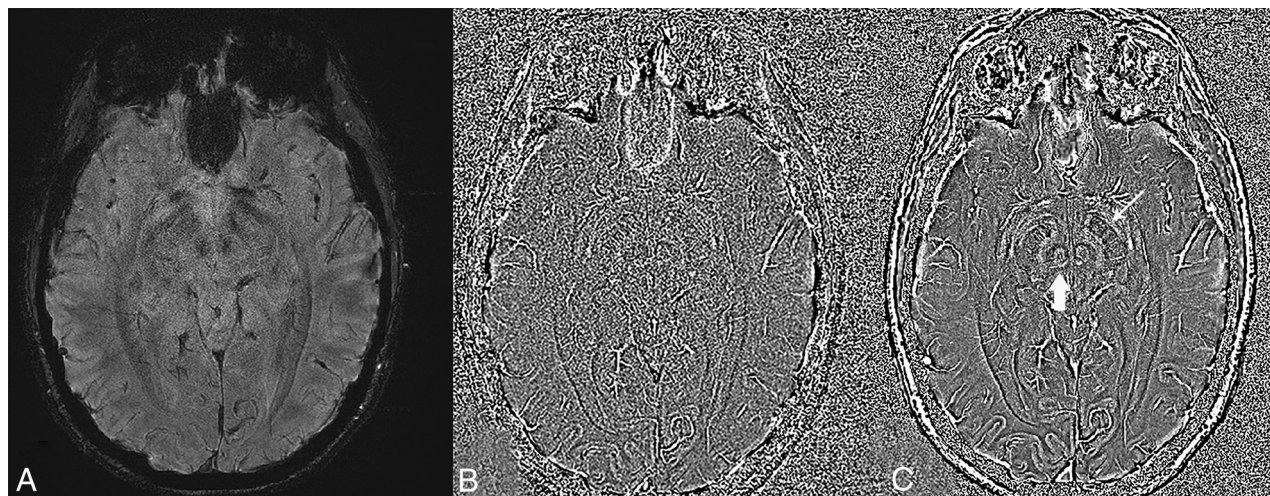


FIG 3. Magnitude (A) and high-pass-filtered phase images obtained from the MAGPI sequence and processed with traditional SWI (B) and MAGPI (C) to highlight the potential of MAGPI processing to capture the optimal phase SNR/contrast-to-noise ratio. Note the overall improved image quality and delineation of structural details seen on MAGPI (C), such as the red nucleus (*vertical arrow*) and substantia nigra (*oblique arrow*).

reduces the need for phase unwrapping because the high-pass-filtering operation applied in complex domains reduces the dynamic range of the underlying phase signal.²⁸ Nevertheless, phase unwrapping can be helpful in regions with a large magnetic susceptibility gradient where the large number of wraps is not resolved with the homodyne-filter operation alone.²⁸ The susceptibility-induced signal loss in those regions reduces the efficacy of phase unwrapping, however. Finally, phase unwrapping often results in inconsistent or incorrect estimates of the underlying phase, with different algorithms often yielding approximate and inconsistent solutions, each with their own advantages and disadvantages.^{11,19}

Our study has several limitations: first, the small sample size that can limit the power and generalizability of our results. Second, due to the study design and inclusion of patients with mTBI, we did not have CMB in deeper structures of the brain that are usually seen with more severe head trauma, often related to diffuse axonal injury. Some of our participants had cerebral contusions near the skull base structures where artifacts are common. However, having a longitudinal design and 3 sequential MR imaging studies helped and allowed the neuroradiologist to resolve any uncertainties about artifacts versus true CMB by examining the longitudinal data. Another potential limitation of this study is the absence of histopathology to confirm the true nature of detected CMB, though this is a common limitation related to a study of this type. The SWI and MAGPI sequences used in this study had slightly different spatial resolutions. The SWI protocol is a standard high-resolution protocol used in clinical scans with a section thickness of 1.2 mm to reduce susceptibility artifacts. However, the SWI still had substantial susceptibility artifacts near the skull base and inferior frontal lobes, which interfered with the diagnostic ability to confidently detect CMB. Despite its thicker section (2 mm), MAGPI-SWI was able to achieve improved susceptibility-induced dephasing artifacts throughout the brain compared with the traditional SWI process.

CONCLUSIONS

Optimal phase unwrapping with reduced susceptibility in MAGPI-SWI can clarify small microbleeds that can go undetected with routinely used conventional SWI.

Disclosures: Kambiz Nael—UNRELATED: Board Membership: Olea Medical, Comments: Medical Advisory Board. Joseph C. Dagher—UNRELATED: Patents (Planned, Pending or Issued): Inventor of the patented MAGPI technology, Comments: patent: MRI with Reconstruction of MR Phase Image; US patent 10,145,925; owner/applicant: Arizona Board of Regents, the University of Arizona. David Millward—RELATED: Grant: University of Arizona, Comments: cost of the MRI use time, research assistant salary to collect data and administer the MRI.*
*Money paid to the institution.

REFERENCES

- Centers for Disease Control and Prevention. Surveillance Report of Traumatic Brain Injury-related Emergency Department Visits, Hospitalizations, and Deaths—United States, 2014. 2019. https://www.cdc.gov/traumaticbraininjury/pdf/TBI-Surveillance-Report-FINAL_508.pdf. Accessed March 29, 2019
- Thurman DJ, Alverson C, Dunn KA, et al. Traumatic brain injury in the United States: A public health perspective. *J Head Trauma Rehabil* 1999;14:602–15 [CrossRef Medline](#)
- Xi G, Keep RF, Hoff JT. Mechanisms of brain injury after intracerebral haemorrhage. *Lancet Neurol* 2006;5:53–63 [CrossRef Medline](#)
- Hughes DG, Jackson A, Mason DL, et al. Abnormalities on magnetic resonance imaging seen acutely following mild traumatic brain injury: correlation with neuropsychological tests and delayed recovery. *Neuroradiology* 2004;46:550–58 [CrossRef Medline](#)
- Scheid R, Preul C, Gruber O, et al. Diffuse axonal injury associated with chronic traumatic brain injury: evidence from T2*-weighted gradient-echo imaging at 3 T. *AJNR Am J Neuroradiol* 2003;24:1049–56 [Medline](#)
- Fazekas F, Kleinert R, Roob G, et al. Histopathologic analysis of foci of signal loss on gradient-echo T2*-weighted MR images in patients with spontaneous intracerebral hemorrhage: evidence of microangiopathy-related microbleeds. *AJNR Am J Neuroradiol* 1999;20:637–42 [Medline](#)
- Goos JD, van der Flier WM, Knol DL, et al. Clinical relevance of improved microbleed detection by susceptibility-weighted magnetic resonance imaging. *Stroke* 2011;42:1894–1900 [CrossRef Medline](#)
- Greenberg SM, Vernooij MW, Cordonnier C, et al; Microbleed Study Group. Cerebral microbleeds: a guide to detection and interpretation. *Lancet Neurol* 2009;8:165–74 [CrossRef Medline](#)
- Uetani H, Hirai T, Hashimoto M, et al. Prevalence and topography of small hypointense foci suggesting microbleeds on 3T susceptibility-weighted imaging in various types of dementia. *AJNR Am J Neuroradiol* 2013;34:984–89 [CrossRef Medline](#)
- Haller S, Montandon ML, Lazeyras F, et al. Radiologic-histopathologic correlation of cerebral microbleeds using pre-mortem and post-mortem MRI. *PLoS One* 2016;11:e0167743 [CrossRef Medline](#)
- Dagher J, Nael K. MAGPI: a framework for maximum likelihood MR phase imaging using multiple receive coils. *Magn Reson Med* 2016;75:1218–31 [CrossRef Medline](#)
- Wu B, Li W, Avram AV, et al. Fast and tissue-optimized mapping of magnetic susceptibility and T2* with multi-echo and multi-shot spirals. *Neuroimage* 2012;59:297–305 [CrossRef Medline](#)
- Dagher J, Nael K. MR phase imaging with bipolar acquisition. *NMR Biomed* 2017;30: [CrossRef Medline](#)
- Haacke EM, Xu Y, Cheng YC, et al. Susceptibility-weighted imaging (SWI). *Magn Reson Med* 2004;52:612–18 [CrossRef Medline](#)
- McPhee KC, Denk C, Al-Rekabi Z, et al. Bilateral filtering of magnetic resonance phase images. *Magn Reson Imaging* 2011;29:1023–29 [CrossRef Medline](#)
- Fine MS, Lum PS, Brokaw EB, et al. Dynamic motor tracking is sensitive to subacute mTBI. *Exp Brain Res* 2016;234:3173–84 [CrossRef Medline](#)
- Cordonnier C, Potter GM, Jackson CA, et al. Improving interrater agreement about brain microbleeds: development of the Brain Observer MicroBleed Scale (BOMBS). *Stroke* 2009;40:94–99 [CrossRef Medline](#)
- Chen JK, Johnston KM, Collie A, et al. A validation of the post concussion symptom scale in the assessment of complex concussion using cognitive testing and functional MRI. *J Neurol Neurosurg Psychiatry* 2007;78:1231–38 [CrossRef Medline](#)
- Keenan KE, Berman BP, Carnicka S, et al. Validating the acquisition and phase estimation process for magnetic susceptibility measurement. In: *Proceedings of the 5th International Workshop on MRI Phase Contrast & Quantitative Susceptibility Mapping*, Seoul, Korea. September 25–28, 2019
- Schrag M, Greer DM. Clinical associations of cerebral microbleeds on magnetic resonance neuroimaging. *J Stroke Cerebrovasc Dis* 2014;23:2489–97 [CrossRef Medline](#)
- Scheid R, Walther K, Guthke T, et al. Cognitive sequelae of diffuse axonal injury. *Arch Neurol* 2006;63:418–24 [CrossRef Medline](#)
- Ayaz M, Boikov AS, Haacke EM, et al. Imaging cerebral microbleeds using susceptibility weighted imaging: one step toward detecting vascular dementia. *J Magn Reson Imaging* 2010;31:142–48 [CrossRef Medline](#)
- Schweser F, Sommer K, Deistung A, et al. Quantitative susceptibility mapping for investigating subtle susceptibility variations in the human brain. *Neuroimage* 2012;62:2083–2100 [CrossRef Medline](#)

24. Tong KA, Ashwal S, Holshouser BA, et al. **Hemorrhagic shearing lesions in children and adolescents with posttraumatic diffuse axonal injury: improved detection and initial results.** *Radiology* 2003;227:332–39 [CrossRef Medline](#)
25. Nandigam RN, Viswanathan A, Delgado P, et al. **MR imaging detection of cerebral microbleeds: effect of susceptibility-weighted imaging, section thickness, and field strength.** *AJNR Am J Neuroradiol* 2009;30:338–43 [CrossRef Medline](#)
26. Wang X, Wei XE, Li MH, et al. **Microbleeds on susceptibility-weighted MRI in depressive and non-depressive patients after mild traumatic brain injury.** *Neurol Sci* 2014;35:1533–39 [CrossRef Medline](#)
27. Huang YL, Kuo YS, Tseng YC, et al. **Susceptibility-weighted MRI in mild traumatic brain injury.** *Neurology* 2015;84:580–85 [CrossRef Medline](#)
28. Li N, Wang WT, Sati P, et al. **Quantitative assessment of susceptibility-weighted imaging processing methods.** *J Magn Reson Imaging* 2014;40:1463–73 [CrossRef Medline](#)